

## Investigation of the Effect of a Flocculent of Bentonite Clay with $MgCO_3$ in Synthetic Acid Mine Drainage (AMD) Treatment

\*Oupa I. Ntwampe and K. Moothi

Department of Chemical Engineering, University of Johannesburg, Doornfontein 2028, Johannesburg, SOUTH AFRICA

**Article history:** Received in revised form Jan. 20, 2018

Accepted Jan. 30, 2018

Available online June 20, 2018

**Cite this article as:** Ntwampe OI and Moothi K. *Investigation of the Effect of a Flocculent of Bentonite Clay with  $MgCO_3$  in Synthetic Acid Mine Drainage (AMD) Treatment.* J Applied Chem. Sci. 2018, 5(2):435-444

DOI : <https://dx.doi.org/10.22341/jacs.on.00501p435>

p-ISSN: 2089-6328, e-ISSN: 2580-1953 © 2018 JACSONline GP. All right served



The JACSONline Group Publisher publishes the work of Jacson-Journal of Applied Chemical Science eISSN: 2580-1953/pISSN: 2089-6328 under the licensing of a [Creative Commons Attribution-NonCommercial-ShareAlike 3.0 Unported License](https://creativecommons.org/licenses/by-nc-sa/3.0/). Authors retain the copyright to their work. Users may read, copy, and distribute the work in any medium provided the authors and the journal are appropriately credited. The users may not use the material for [commercial purposes](#).

### ABSTRACTS

Effect of a flocculent of bentonite clay with  $MgCO_3$  in Synthetic AMD was investigated in present study. The AMD samples were collected from the western decant in Krugersdorp, South Africa was modified by adding arsenic, zinc and cobalt. The pH, conductivity, dissolved oxygen (DO), oxygen reduction potential (ORP) and turbidity were measured. Those samples were treated with bentonite clay,  $MgCO_3$  and a flocculent of bentonite clay and  $MgCO_3$  respectively in a jar test, employing either rapid or slow mixing. Results showed that the conductivity of the samples with increasing bentonite clay while keeping  $MgCO_3$  constant decreased with increasing dosage, which was attributed to adsorption of the ions onto the negative sites of the porous bentonite when ionic strength increased. The oxygen content of the DO and ORP was not influenced by the rate of mechanical agitation, i.e. rapid and slow mixing respectively. Destabilization-hydrolysis was not influenced by the pH but the ionic strength of the colloidal AMD suspension, valence and electronegative of the metal ions. Turbidity removal of the synthetic flocculent used occurred through physico-chemical phenomenon (SEM micrographs) and charged porous bentonite clay. **In conclusion:** Bentonite clay controls equilibrium state of the ionic strength of the system through adsorption of excess ions added to the system. Velocity gradient induced by mechanical agitation does not have an influence on the turbidity removal.

**Keywords:** wastewater, coagulants, AMD, mixing, shaking, turbidity

\* Corresponding author: [ontwampe@gmail.com](mailto:ontwampe@gmail.com)

### 1. Introduction

The major environmental degradation attributed to mining operations world-wide includes uncontrolled discharge of contaminated decant from abandoned mines (Pulles *et al.*, 2005), which is commonly termed AMD. The type of wastewater is characterized by low pH, high salinity, elevated concentration of sulphate, iron, aluminum and manganese, among others. It also contains high level of toxic heavy metals such as cobalt, copper, cadmium, zinc including radionuclides (Akciil *et al.*, 2006). AMD is not only associated with surface and groundwater contamination, but also degrade soil quality, aquatic habitats and allows seepage of heavy metals into the environment (Adler *et al.*, 2007). It is also detrimental to humans as it poses threat to human life due to its high heavy metals which are non-biodegradable. They accumulate in living organisms causing various diseases and disorders (Nagajyoti *et al.*, 2010). Low pH of AMD results in solubility of heavy metals in water and the high concentration is an attribute to toxicological effects on aquatic systems (Nagajyoti *et al.*, 2010). Acidic water rich in metals may also form in spoil heaps and mineral tailings through biological processes as in the mines, but the quality of the AMD derived from those sources may be more aggressive compared to those discharged from the mines. However, both types of AMD originate from mining operations except that the latter is formed from the

sulphuric acid which is produced during the oxidation of pyrite, a precursor to AMD. The sulphuric acid evaporates to the atmosphere and is introduced to the tailings and surface during rainfall. The impact of the mining waste, especially AMD is so catastrophic.

Environmental Protection Agency (1987) revealed that catastrophic may be rated as the second to global warming and stratospheric ozone depletion in terms of ecological risk. Polluted sites may not be fully rehabilitated or restored as pollution is so persistent that there prevails no effective remedy (EEB, 2000). South Africa is one of the countries with multiple mining operations, gold and coal mining, the main sources of AMD being predominant. Catastrophic decant started in the West Rand (Goldfields) in August 2002, where it flowed northwards through the game reserve towards Cradle of Humankind World Heritage Site, causing a serious damage (Oelofse *et al.*, 2007). The incident caused a chaos especially the blame which was directed to the scientists, mining companies and government for their reluctance to initiate remediation action towards AMD decant (Mail & Guardian, 2005).

Treatment of AMD is a serious challenge as it is costly and requires sophisticated technologies, thus orchestrating negligence towards AMD treatment approach. Although that would be economical especially during the current water-

scarcity crisis which is attributed climate change, treatment costs still remain unbearable. Conventional wastewater treatment using inorganic coagulants has widely been employed for some time due to abundance of Fe and Al on the earth crust. The technique is simple and cost-effective as it involves coagulation-flocculation process. The efficiency of coagulation-flocculation strongly affects the overall treatment performance (Bratby, 2016), hence it is essential to optimize dosage to achieve optimal destabilization-hydrolysis; the stage where coagulation-flocculation occurs.

Coagulation-flocculation is a process which is divided into two distinct processes, i.e. the former being the process where destabilization of a colloidal suspension occurs to overcome stability of the system. The latter is explained as the induction of the destabilized particles in order to agglomerate so that separation through gravity settling can be accomplished.

Coagulation-flocculation is determined by the rate of destabilization-hydrolysis, which is attributed to the ability of the coagulant to disrupt equilibrium between the van der Waals attractive and electrostatic repulsive forces, diffusing through the electrical double layer (EDL) of the aqua-colloids (Sincero *et al.*, 2003). According to Debye-Hückel theory, it is possible to calculate that the thickness of this layer is given by the equation:

$$Z = 0.33 \times 10^{-2} \sqrt{\epsilon / I} \quad (1)$$

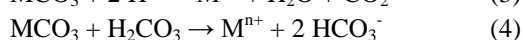
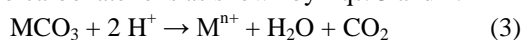
where  $z$  = thickness of layer, in cm,  $\epsilon$  = dielectric constant for the solution (C/V.cm) and  $I$  = ionic strength, in mol/L

The results from Eq. 1 indicate that EDL repression is achieved by increasing the ionic strength of the solution. Increasing the ionic strength of the solution through addition of more ionic species and adding ions of high valence is expressed as:

$$I = 0.5 \sum C_j Z_j^2 \quad (2)$$

where  $C$  = concentration of ionic species  $j$ ,  $Z$  = charge of ionic species  $j$

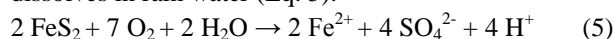
Apart from conventional treatment, neutralization of the AMD sample using metal hydroxide was also employed during AMD treatment. Researchers such as Aubè *et al.*, (2003), Maree (2004), Akcil *et al.* (2006) and Kurniawan *et al.* (2006) employed lime neutralization for the removal of heavy metals and sulphates. Neutralizing reagents react with the hardness and natural alkalinity in the wastewater to form insoluble compounds, which then precipitate and are removed from the water by sedimentation and, usually, filtration. Inevitably, neutralizing reagents are more appropriate in AMD treatment as they may consume the protons and add alkalinity through bicarbonate ions as shown by Eqs. 3 and 4.



where  $M = \text{Mg}$ .

In the case of raw water supply, neutralizing reagents are added to remove hardness which is in the form of temporary (calcium or magnesium bicarbonate) and permanent

(chloride or sulphate ions) hardness. The former originates from the dissolution of naturally occurring salts in rain water whereas the latter is derived from mineral acids present in rain water or the solution of naturally occurring acidic minerals. A fraction of sulphate ions is derived from the oxidation of pyrite (AMD formation) which evaporated to the atmosphere and dissolves in rain water (Eq. 5).



Apart from inorganic and neutralizing reagent, clay has been used in the treatment of the AMD (Dzombak *et al.*, 1995, Ekosse *et al.*, 2010, Gitari *et al.*, 2011, Otto *et al.*, 2013, Emmanuel *et al.*, 2013, Mansri *et al.*, 2015, Ntwampe *et al.*, 2015a and 2015b), among others. The advantage of using clay in the treatment of AMD is its pH-independent adsorption property of metals which is attributed to cation exchange in the interlayers and the electrostatic interaction between the ions and the permanent charge (Dzombak *et al.*, 1995). Furthermore, adsorption by ion exchange is predominant at low ionic strength and pH, where the latter relates to the wastewater (AMD) treated in this study. The process can be explained by Donnan equilibrium or the accumulation of ions in the double layers which develop at the basal planes of the clay lamellae (Dzombak *et al.*, 1995). Donnan equilibrium expresses clay particles as separate homogeneous phases bearing negative charges arising from isomorphous substitution. On the other hand, the ion exchange reaction (e.g.  $\text{Na}^+$  and  $\text{H}^+$ ) is expressed as:



where  $X$  = solid exchanger,  $\text{H}^+$  and  $\text{Na}^+$  = ions in solution and  $K_e$  = mass action law coefficient for the reaction.

Bentonite clay which is mined in South Africa generally contains both calcium and magnesium montmorillonite (Nel *et al.* 2014). Clay has previously been evaluated as a reagent for turbidity adsorption (Tahir *et al.*, 2007, Waanders *et al.*, 2010, Gitari *et al.*, 2011 and Ntwampe *et al.*, 2016). Montmorillonite has a large specific surface area with a net specific charge and is responsible for bentonite's large exchange capacity (Syafalni *et al.* 2013). Montmorillonite is composed of a central sheet of octahedral aluminium ions between two tetrahedral sheets (T-O-T) of silicon ions; these sheets are linked by oxygen atoms. The configuration of the bentonite clay is responsible for its efficiency in adsorption/absorption (Syafalni *et al.*, 2013).

$\text{MgCO}_3$ , the reagent which is used in this study is not popularly employed during wastewater treatment. However, the choice to use it in the treatment of the AMD in this study is based on the similarity between calcium and magnesium ions, i.e. they are metalloids, identical valence and electronegativity, but different electron configuration. It exhibits similarly identical reactivity with calcium ion during water softening (Eqs. 1 and 2). On the other hand, the flocculent prepared by the combination of bentonite clay and  $\text{MgCO}_3$  is perceived to yield optimal turbidity removal.

The present study investigates the capacity of the adsorption of the combination of bentonite clay and  $\text{MgCO}_3$

dosage from the AMD sample, a significant factor in wastewater treatment. Initial concentration of the adsorbate determines the adsorption capacity of an adsorbent (Ouazene, 2010), hence it is significant to use a cost-effective reagent/adsorbent (flocculent). Percentage turbidity removal efficiency (E %) is calculated in the Eq. 7.

$$E \% = \frac{C_0 - C_i}{C_0} \times 100 \quad (7)$$

where  $C_0$  and  $C_i$  = initial and residual concentration of the wastewater effluent (mg/L), respectively.

The adsorption capacity at different times has to be calculated according to afore-mentioned equation. Pseudo first-order is expressed by Eq. 8:

$$\frac{dq_t}{dt} = k_1(q_e - q_t) \quad (8)$$

The pseudo second-order can be described by Eq. 9:

$$\frac{dq_t}{dt} = k_2(q_e - q_t)^2 \quad (9)$$

where  $q_e$  = the adsorbed amount of the dye at equilibrium (mg/g),  $q_t$  = the adsorbed amount of dye at a certain time  $t$  (mg/g) and  $k_1$  and  $k_2$  = the rate constant for the first and second order adsorption kinetics, respectively. These kinetic modeling were required to report the rate of adsorptions.

The main objective of this study is to determine turbidity removal efficiency of a combination of bentonite clay and magnesium carbonate (flocculent) in AMD treatment without pH adjustment. The other objectives include the determination of the effect of mixing speeds (rapid or slow mixing) and the methods (mixing or shaking) on turbidity removal from AMD treatment with a combination of using bentonite clay and magnesium carbonate dosage.

## 2. Materials and Methods

In this study, coagulation-flocculation treatment has been applied to the AMD sample using 20-60 mL dosages of varying masses (0.5-2.5 g) of bentonite clay and 0.043 M  $Mg^{2+}$  in  $MgCO_3$ , respectively, prepared with demineralized water. The study also includes the optimization of the dosage (increasing bentonite clay while decreasing  $MgCO_3$ ). A second study includes the determination of the effect of mixing speed while the third study determines the effect of turbidity removal efficiency between mixing and shaking. The pH, conductivity, turbidity, DO and ORP of the samples were measured before and 1 hour after each set of experiments. A 200 mL AMD sample was poured into 500 mL glass beakers or Erlenmeyer flasks and 20, 30, 40, 50 and 60 mL of a reagent was poured respectively, mixed in a flocculator or a shaker at 250 rpm for 2 minutes and reduced to 80 rpm for 10 minutes. The samples were allowed to settle for 1 hour after which the measurements were conducted. Another similar set of experiments was conducted to compare the effect of rapid with slow mixing in the AMD treatment with bentonite clay and  $MgCO_3$  dosage respectively or as a flocculent.

### 2.1 AMD sample

The samples were collected from the Western Decant in Krugersdorp in a 25 litres plastic drum. The sample was air-

tied and stored at room temperature. The quality of the sample was modified by adding 3.23, 2.5, 2.8 and 8.9 g/mol of As, Co, Zn and Pb, which have 75, 59, 65 and 207 g/mol, respectively. The pH, conductivity, residual turbidity, ORP, and DO of raw AMD sample were 2.16, 6.27 mS/cm, 207 NTU, 241 mV, and 3.9 mg/L, respectively. The sample contained the following major elements: Cu, Zn, Co, Ni, Mn, Ti, Pb, Al, Fe, Se, Na, Mg, Ca and K, and the concentrations are shown in Table 1.

Table 1: ICP-EOS results of the metals in supernatant of raw AMD

Elements	Concentrations (ppm)
Al	1.182
Ca	173.4
Co	47.6
Cu	0.14
Fe	28.3
K	4.5
Mg	67.3
Mn	35.3
Na	44.5
Ni	0.44
Pb	39.5
As	41.3
Se	0.71
Zn	36.8

### 2.2 Coagulant

Inorganic coagulants of 0.043 M of  $Mg^{2+}$  ions were dosed for coagulation-flocculation of the AMD, and the concentrations are chosen as per a study which was conducted by Ntwampe *et al.* (2013) on paint wastewater treatment. The calculation of the mass of metal salt (Table 2) to obtain 0.043 M of  $M^{n+}$  ( $M^{n+} = Mg$ ) was as follows:

Monoprotic metal salts ( $MCl_3$ )

$$0.043 \text{ M of } M^{3+} \times \text{mass of } M^*CO_3 \cdot 6H_2O \quad (M^* = Mg) \quad (10)$$

Table 2. Mass of  $MgCO_3$  for the preparation of standard solutions

Salt	Mass of salt (g)	Conc <sup>n</sup> (mol/L)	$M^{3+}$ conc <sup>n</sup> (M)
$MgCO_3$	2.49	0.043	0.043

### 2.3 Procedure in jar tests or a shaker.

The equipment used for the jar tests was a *BIBBY Stuart Scientific Flocculator (SW1 model)*, which has six adjustable paddles with rotating speeds between 0–350 rpm. 200 mL sample of AMD containing 11.9 g of solid particles was poured into each of the five 500 mL glass beakers or Erlenmeyer flasks for the test. Rapid mixing was set at 250 rpm for 2 minutes, followed by slow mixing at 80 rpm for 10 minutes, a normal standard recommended in a jar test.

### 2.4 Performance evaluation

The pH was used as a determinant to assess the rate of hydrolysis and hydrolytic potential of bentonite clay and  $MgCO_3$  flocculent at different mixing duration, whereas the concentration and turbidity were measured to determine the ionic potential and removal of colloidal particles from the samples respectively.

#### 2.4.1 pH/ORP/DO/CD measurements

A Senso Direct Multimeter (*made in South Africa*) was used to measure the pH/ORP/DO/CD with an electrode filled with silver chloride solution and the outer glass casing

membrane covering at the tip was used. The equipment was calibrated with standard solutions with pH of 4.0 and 7.0 before use. Each parameter used its probe which was replaced prior to measurements, and an appropriate selection button was pressed to measure the correct parameter.

#### 2.4.2 Turbidity measurement

A Merck Turbiquant 3000T Turbidimeter (*made in Japan*) was used to determine turbidity or the suspended particles in the supernatant, using NTU as a unit of measure. It was calibrated with 0.10, 10, 100, 1000 and 10000 NTU standard solutions. The values obtained were multiplied by 2.4 to convert to TSS (g/L).

#### 2.4.3 Scanning Electron Microscopic Analysis

A KYKY-EM3200 digital scanning electron microscope (model EM3200) equipment (China) was used to produce the SEM photomicrographs.

#### 2.4.4 Inductively Coupled Plasma (ICP-OES)

A Perkin Elmer Optima DV 7000 ICP-OES optical emission spectrometer (USA) was used to determine the metals in the supernatant of the AMD samples. It was calibrated with a standard solution between 2-50 mg/L of the salts mentioned above.

### 3. Results and Discussion

#### 3.1. DO Concentration and ORP

The DO and ORP were measured to determine the concentrations of oxygen and redox potential, respectively. Data reported on Fig. 1 represents the AMD sample with increasing dosage (0.5, 1.0, 1.5, 2.0 and 2.5 g) of bentonite clay and decreasing dosage (60, 50, 40, 30 and 20 mL) of  $MgCO_3$ , and vice versa; on the other hand, increasing or decreasing dosage of a combination of bentonite clay and  $MgCO_3$ .

The changing pH during destabilization-hydrolysis is indicative of the rate of hydrolysis, i.e. dehydroxylation of the hydration spheres of hexagonally hydrated central metal ion to form hydrolysis species releasing protons. The protons released are attributable to the changing (decreasing) pH of the solution. The stability of a colloidal suspension which is caused by the formation of EDL prevents agglomeration. It is dependent upon the surface charge of the colloidal suspension and the composition of the solution, i.e. the pH and ionic strength. (Geckeis *et al.*, 2011 and Schelero *et al.*, 2011). It is destroyed when a reagent with high valence and electronegativity is added, causing destabilization-hydrolysis and agglomeration. The reaction is faster when the colloidal suspension has high ionic strength and charge density (Deepthi *et al.*, 2011 and Loux, 2011), an observation revealed by the changing pH with increasing dosage of a flocculent (Fig. 1), i.e. higher rate of destabilization-hydrolysis (Environmental contamination by anthropogenic radionuclides through ground water). Inevitably, ineffective destabilization-hydrolysis is indicative of a weak reagent as it is incapable of diffusing throughout the EDL to disturb the equilibrium between the van der Waals attractive and electrostatic repulsive forces (Swartz

*et al.*, 2004). The coagulants with their cations ( $M^{n+}$ ) proliferate the concentration of the positive charges in the system, thus weakening the electrostatic forces of repulsion. The metal ions of the coagulants in the polarized system are then hydroxylated to form precipitates which are sorption substrates.

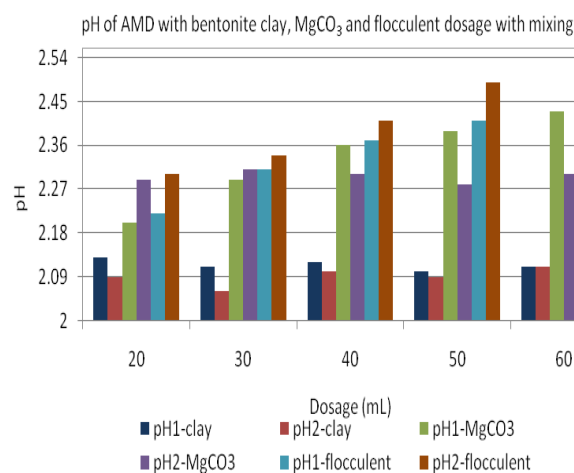


Fig. 1. pH of AMD with bentonite clay,  $MgCO_3$  and flocculent dosage with mixing

$pH_1$ -clay = pH of increasing clay,  $pH_2$ -clay = pH of decreasing clay,  $pH_1$ - $MgCO_3$  = pH of increasing  $MgCO_3$ ,  $pH_2$ - $MgCO_3$  = pH of decreasing  $MgCO_3$ ,  $pH_1$ -flocculent = pH of increasing clay and constant  $MgCO_3$  and  $pH_2$  = pH of increasing  $MgCO_3$  and constant clay. (Clay = bentonite clay)

The pH of the AMD samples with increasing bentonite clay dosage (Fig. 1) does not exhibit strongly change, i.e. 2.16 in the raw AMD to a range of 2.10-2.13. The results indicate that the clay does not undergo hydrolysis. Similarly, the pH of the AMD samples with decreasing dosage does not exhibit any change, in a range of 2.09-2.11. The pH of increasing dosage of  $MgCO_3$  exhibits an increasing trend in a range of 2.10-2.43. On the other hand, the pH of decreasing dosage of  $MgCO_3$  increases slightly in a range of 2.29-2.30. The reason for a change of 2.29, 2.31 and 2.30 in the samples with 60, 50 and 40 mL respectively is attributed to the small amount of bentonite clay added, i.e. 0.5, 1.0 and 1.5 g, respectively.

The pH of the samples with increasing bentonite clay and a constant  $MgCO_3$  (Fig. 1) increases in a range of 2.22-2.40, while the pH of the samples with increasing  $MgCO_3$  and constant bentonite clay increases considerably in a range of 2.30-2.56. The slight increasing trend of the pH of the samples with constant  $MgCO_3$  is attributed to the increasing concentration with increasing quantity of the flocculent. This is invoked by considerable pH change with increasing  $MgCO_3$  and constant bentonite clay (2.30-2.54), which also shows the neutralizing potential of  $MgCO_3$ .

The rising pH shows that the  $MgCO_3$  dissolved to form  $Mg^{2+}$  and  $CO_3^{2-}$ , where the former hydrolysed to form  $Mg(OH)^+$  and  $Mg(OH)_2$  whereas the latter remained suspended in the solution. The formation explains that turbidity removal is through particle bridging and entrapment in the precipitate ( $Mg(OH)_2(s)$ ).

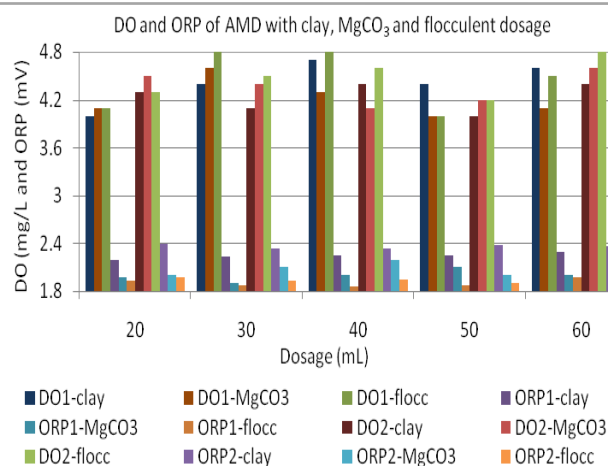


Fig. 2. DO and ORP of AMD with bentonite clay,  $MgCO_3$  and flocculent dosage with mixing

$DO1/ORP1 = DO/ORP$  with rapid mixing,  $DO2/ORP2 = DO/ORP$  with slow mixing and flocc = combination of bentonite and  $MgCO_3$ .

The experimental results (Fig. 2) showed an insignificant change between the raw and treated AMD on the former, i.e. from 3.9 mg/L to the ranges of 4.0-4.8 mg/L (rapid mixing) and 4.0-4.8 mg/L (slow mixing), whereas changed from 236 mV to the ranges of 188-229 mV (rapid mixing) and 189-237 mV (slow mixing). The lower variation of the DO between the raw and treated AMD sample is indicative of a limited or no oxidation in the system and vice versa. On the other hand, the upper limit of the ORP of the samples with slow mixing exhibits a slight higher value than the rapid mixing, the positive value is indicative of predominance of reduction reaction.

In view of the fact that the DO and ORP reflect the concentration of the oxygen which is utilized for oxidation-reduction (redox) reaction, the results are indicative of redox. According to Table 1, it shows that oxygen was utilized during redox reaction of heavy metals to form active cations some of which react to form precipitates. The DO of the samples with bentonite clay and  $MgCO_3$  does not exhibit discrepancy compared to the raw AMD sample. In addition, the DO of those samples treated during rapid and slow mixing do not exhibit discrepancy, which indicates that redox reaction is not influenced by the rate of mechanical agitation. On the contrary, the DO of the samples with a combination of bentonite clay and  $MgCO_3$  exhibited a slight change, which is indicative of redox reaction. In general, the DO and ORP between the samples with rapid mixing do not exhibit a difference compared to their corresponding samples with slow mixing. Although the discrepancy of the DO and ORP between the raw and treated AMD samples does not change, the observations in the present study indicate that they are not influenced by the rate of mechanical agitation (Fig. 2).

Fig. 3 represents the conductivity and residual turbidity of the samples with bentonite clay,  $MgCO_3$  and a combination of bentonite clay and  $MgCO_3$ , respectively while increasing and decreasing their concentrations interchangeably.

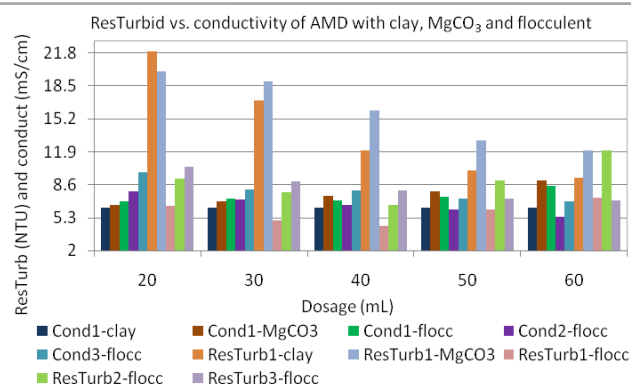


Fig. 3. Conductivity vs. residual turbidity of AMD with bentonite clay,  $MgCO_3$  and flocculent dosage with mixing

$Cond1 =$  conductivity,  $cond2-flocc =$  conductivity of flocculent with increasing clay and decreasing  $MgCO_3$ ,  $cond3-flocc =$  conductivity of flocculent with increasing  $MgCO_3$  and constant clay,  $ResTurb1 =$  residual turbidity,  $ResTurb2-flocc =$  residual turbidity of flocculent with increasing clay and constant  $MgCO_3$ ,  $ResTurb3-flocc =$  residual turbidity of flocculent with increasing  $MgCO_3$  and constant clay. (Clay = bentonite clay).

The conductivity is an indicative of the total ions in the colloidal suspension, i.e. positively charged cations ( $H^+$ ,  $Na^+$ ,  $Mg^{2+}$ , etc.) and negative anions ( $OH^-$ ,  $Cl^-$ ,  $SO_4^{2-}$ , etc.). The conductivity is attributed to the ionizable compounds when remaining unreactive and thus suspended in the solution; and therefore directly proportional to the concentration of the ions. The ions are in Brownian motion but at different velocities (mobilities) through the solution, contributing differently to the conductivity. The common cations with high mobility include the hydrogen ions [ $H^+$ ] whereas the anions with high mobility are the hydroxyl ion [ $OH^-$ ].

The conductivity of the samples with increasing bentonite clay (Fig. 3) does not exhibit significant change compared to conductivity of the raw AMD, whereas the conductivity of the samples with increasing  $MgCO_3$  and flocculent increases with dosage. The discrepancy of the conductivity between the samples with  $MgCO_3$  and flocculent is almost similar, which correlate to conductivity of the samples with bentonite clay only. The observation confirms that bentonite clay does not have an effect on the conductivity of the AMD. On the hand, conductivity of the samples with increasing bentonite clay while keeping  $MgCO_3$  constant decreases with increasing dosage. This may be attributed to adsorption of dissolved ions onto the negative sites of the porous bentonite when ionic strength increases. This trend is also prevalent in the samples with increasing  $MgCO_3$  and constant bentonite clay, which indicates that the system reached a saturation point resulting to adsorption of excess ions onto the bentonite clay.

The residual turbidity of the samples with increasing bentonite clay (Fig. 3) decreases with increasing concentration from 207 NTU (raw AMD) to a range of 22-9.3 NTU, showing that there are more pore sites for adsorption with increasing concentration. Similarly, residual turbidity of the samples with  $MgCO_3$  decreases with dosage, which is indicative of ameliorated neutralization with increasing dosage. Turbidity

below 15 NTU is considered as within the specification while below 20 NTU as moderate in the present study. Neutralization is exhibited by the reduced concentration of the heavy metals (Table 3) to form settleable precipitates. However, the precipitates are not directly formed from the decomposition of the  $MgCO_3$ , but through hydroxylation (Eq. 11) and the reaction of metal ions with amphoteric water molecules of the bulk fluid (Eqs.12 and 13)

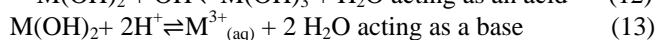
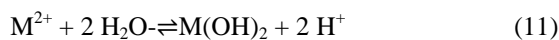


Table 3. ICP-EOS results of the metals in supernatant of treated AMD

Elements	Concentrations (ppm)
Al	1.175
Ca	67.3
Co	1.56
Cu	0.14
Fe	16.1
K	4.1
Mg	42.5
Mn	8.6
Na	34.2
Ni	0.44
Pb	3.6
As	4.93
Se	0.68
Zn	4.3

Eq. 9 shows that hydroxylation of a metal ion in a solution is spontaneous due to acid-base property of water molecules, which is also attributed to their bipolarity. The reduced heavy metals (Table 3) include Fe, Ca, Co, Mg, Mn, Na, As and Zn, some of which are hydroxylated ( $M(OH)_2$ ) and settle as precipitates when others are sorbed onto the  $Mg(OH)_2$  precipitates. Some heavy metal ions are adsorbed onto the charged sites of the porous bentonite clay when the others are intercalated between the T-O-T layers of the bentonite clay. The net negative charge of the bentonite clay as a result of cationic substitution within T-O-T (Oladipo *et al.*, 2014) enables it to attract the metal ions (Table 3). Excitingly, the flocculent used in this study exhibited a degree of heavy metals removal, i.e. As, Co, Zn and Pb from 41.3, 47.6, 36.8 and 39.4 mg/L to 4.93, 1.56, 4.3 and 3.6 mg/L. This yielded percentage turbid material removal efficiencies of 86.8, 96.7, 88.3 and 90.0 %, these percentage removal efficiencies fall within acceptable limits.

The results shown by residual turbidity (Fig. 3) are in agreement with Eqs. 1 and 2, which express the repression of the EDL with higher ionic strength, i.e. elevated conductivity. The high ionic strength is indicative of high concentration of dissolved ions which induce double layer compression. Double layer compression occurs during diffusion of counterions decreasing the distance between neighbouring particles, which

results in the high rate of collision and agglomeration. As a consequence, adsorption is inevitable resulting in the reduction of the heavy metals and turbid material (Fig. 3).

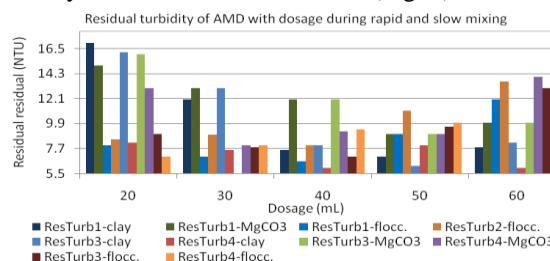


Fig. 4. Residual turbidity of AMD with bentonite clay,  $MgCO_3$  and flocculent dosage with rapid and slow mixing

*ResTurb1* = residual turbidity of increasing, *ResTurb1-flocc* = residual turbidity of increasing clay and constant  $MgCO_3$ , *ResTurb2-flocc* = residual turbidity of increasing  $MgCO_3$  and constant clay, *ResTurb3-clay* = residual turbidity of increasing clay, *ResTurb4-clay* = residual turbidity of decreasing clay, *ResTurb3- $MgCO_3$*  = residual turbidity of increasing  $MgCO_3$ , *ResTurb4- $MgCO_3$*  = residual turbidity of decreasing  $MgCO_3$ , *ResTurb3-flocculent* = residual turbidity of increasing clay and constant  $MgCO_3$  and *ResTurb4* = residual turbidity of increasing  $MgCO_3$  and constant clay. (Clay = bentonite clay, 1 and 2 = rapid mixing, 3 and 4 = slow mixing)

Fig. 4 illustrates residual turbidity of the AMD with bentonite clay,  $MgCO_3$  and flocculent respectively with increasing, decreasing and constant dosages inter changeably, employing rapid and slow mixing. The rationale is to determine the effect of the rate of mechanical agitation (flocculation and flocculation) in the removal of turbidity. As mixing employed in wastewater treatment is applied in two processes, rapid mixing induces high shear forces which result in floc rupture and poor adsorption, whereas flocculation increases adsorption capacity of the turbid material through velocity gradient and differential velocity (Aboulhassan *et al.*, 2006).

Residual turbidity of the samples with increasing bentonite clay and rapid mixing (Fig. 4) decreases with dosage from 207 NTU to a range of 17.0-7.8 NTU, whereas the turbidity of the samples with increasing  $MgCO_3$  exhibits an inconsistent changing trend in a range of 15.0-9.2 NTU. Both reagents exhibit the lowest residual turbidity (7.3-10 NTU) in the samples with 50 and 60 mL dosages, which is expensive compared to 20 and 30 mL dosage in a larger scale. Residual turbidity of the samples with increasing bentonite clay and constant  $MgCO_3$  (flocculent) with rapid mixing is lower compared to the samples with bentonite clay or  $MgCO_3$  dosage, in a range of 6.6-11.8 NTU. The samples with the lower dosages, 20-40 mL yielded the lowest residual turbidity (6.6-8.1 NTU). However, residual turbidity of the samples with increasing  $MgCO_3$  and constant bentonite clay (Fig. 4) yielded slightly higher residual turbidity (8.0-13.6 NTU) than the former set of experiments. The results are more likely to be attributed to the constant bentonite clay dosage, deterring optimal turbidity removal, a condition prevalent in a set of experiments with increasing bentonite clay.

The residual turbidity of the samples with increasing and decreasing dosages of bentonite clay (slow mixing) yielded higher values in the samples with 20-40 mL (16.2-8.1

NTU) whereas the latter yielded residual turbidity in a range of 8.2-6.0 NTU. This is attributed to lower concentration (0.5, 1.0 and 1.5 g/L) compared to 2.5, 2.0 and 1.5 g/L of AMD. Furthermore, the residual turbidity of the samples with increasing and decreasing  $MgCO_3$  dosage (slow mixing) is slightly higher than the set of experiments with bentonite clay, i.e. in the ranges of 9.0-16.3 and 8.7-14.8 NTU, respectively. The results show that bentonite clay has more turbidity removal efficiency than  $MgCO_3$ .

Residual turbidity of the samples with increasing bentonite clay and constant  $MgCO_3$  exhibited an inconsistent changing trend in a range of 7.0-13.4 NTU, where the samples with 30 and 40 mL showing the lowest values. The residual turbidity of the samples with  $MgCO_3$  dosage (slow mixing) exhibited an increasing changing trend in a range of 7.0-12.5 NTU. The changing trend is mainly attributed to increasing concentration of  $MgCO_3$  as bentonite clay is constant. Overall, the residual turbidity of the samples with all the reagents (rapid mixing) is similarly identical to that of the samples with slow mixing, i.e. in the ranges of 6.6-13.6 and 7.0-13.2 NTU respectively. The experimental results show that velocity gradient induced by mechanical agitation does not have an influence on the turbidity removal from the AMD with a combination of bentonite clay and  $MgCO_3$  dosage.

Figs. 5 and 6 represent the correlation between the pH and the efficiencies of turbidity removal in the samples with a combination of bentonite clay and  $MgCO_3$  dosage with rapid and slow mixing, respectively. The object was to determine the accuracy of the data used to plot pH and residual turbidity graphs.

Correlation coefficient between the pH and turbidity removal efficiencies of the combination of bentonite clay and  $MgCO_3$  dosage with rapid mixing (Figs. 1 and 4) is 97.9 %.

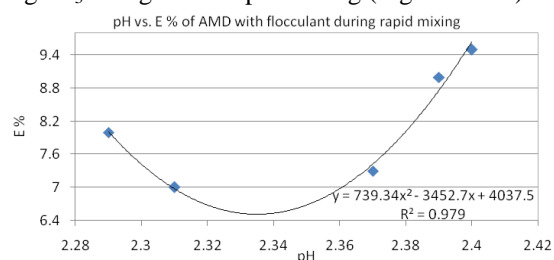


Fig. 5. E % vs. pH of the AMD with a combination of bentonite clay and  $CaCO_3$  rapid mixing

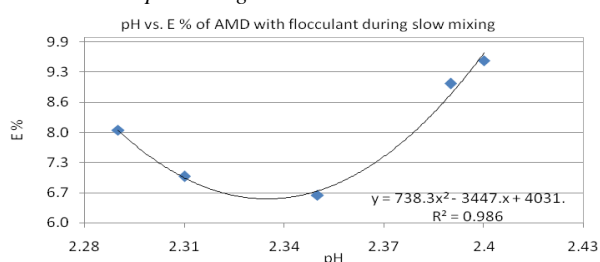


Fig. 6. E % vs. pH of the AMD with a combination of bentonite clay and  $CaCO_3$  slow mixing

Correlation coefficient between the pH and turbidity removal efficiencies of the combination of bentonite clay and  $MgCO_3$  dosage with slow mixing (Figs. 1 and 4) is 98.6 %. Fig. 7 shows the Freundlich model of the AMD sample with a

combination of bentonite clay and  $MgCO_3$  dosage with slow mixing. Statistical analysis (Table A1) validate the accuracy and reliability of the experimental data as already exhibited by the Freundlich model. Statistical analysis was computed using the same sample also with slow mixing.

Table A1: Statistical analysis of the samples with a combination of bentonite clay and  $MgCO_3$  with slow mixing

Expt.1	Expt.2	Av.	A.D.	S.D	% A.D.	C.I.	% E.E	E.E		
1	2.2	2.24	2.22	0.02	0.02	0.9	3.18245	1.4	0.03	2.2 ± 0.15
2	2.29	2.26	2.275	0.02	0.02	0.7	3.18245	1.1	0.02	2.5 ± 0.10
3	2.34	2.31	2.325	0.01	0.01	0.6	3.18245	1.1	0.03	2.1 ± 0.21
4	2.41	2.37	2.39	0.02	0.02	0.8	3.18245	1.5	0.04	2.7 ± 0.69

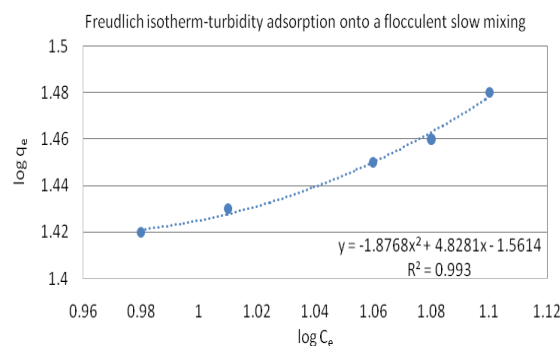


Fig. 7. Freundlich isotherm of turbid material onto a combination of bentonite clay and  $MgCO_3$  with slow mixing

It is observed that the value of the determination coefficient is close to unity (0.993), which implies that the Freundlich model is suitable for the prediction of the adsorption behaviour in this study. It has not been ideal to plot Langmuir model to evaluate an accurate predictive model as commonly done because of the accuracy exhibited by Freundlich model.

The kinetic study using pseudo second order Freundlich model (Eq. 9) was deemed unnecessary as the adsorption variances between intervals (Fig. 6) are insignificant (Table A1). Statistical analysis was computed using the sample with a combination of bentonite clay and  $MgCO_3$  dosage with slow mixing to validate the accuracy and reliability of the experimental data (Table A1).

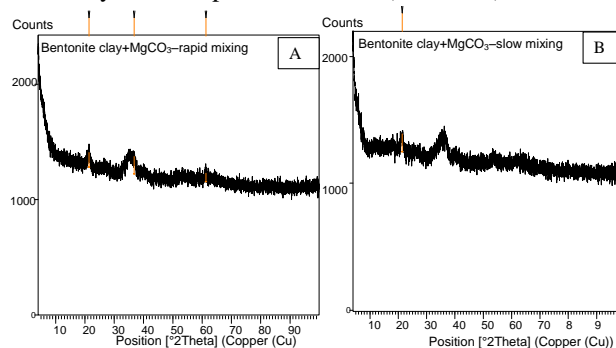


Fig. 8. XRD graphs of the sludge of the AMD with a combination of bentonite clay and  $CaCO_3$  during rapid and slow mixing

The XRD curves (Fig. 8) of the AMD sludge of the samples with a combination of bentonite clay and  $MgCO_3$  dosage with rapid and slow mixing, respectively (Fig. 8). The XRD results of the AMD sludge with a flocculent during rapid mixing (Fig. 8A) shows four peaks representing crystalline materials at  $2\theta$  positions of 20, 37 and a small peaks at 38 and  $61^\circ$ , respectively; with intensity slightly above 1000 and 1700

counts. Similarly, the XRD results of the AMD sludge with a flocculent during slow mixing (Fig. 8B) shows small peak at 21, 37 and two small peaks at 55 and 65° position and same intensity. The peaks indicate that the residual mineral phases retained in the sludge of the AMD samples with a combination of bentonite clay and  $MgCO_3$  rapid and slow mixing are identical.

The SEM micrographs (Fig. 9) show the crystal morphology of the AMD sludge with a combination of bentonite clay and  $MgCO_3$  with rapid and slow mixing, respectively.

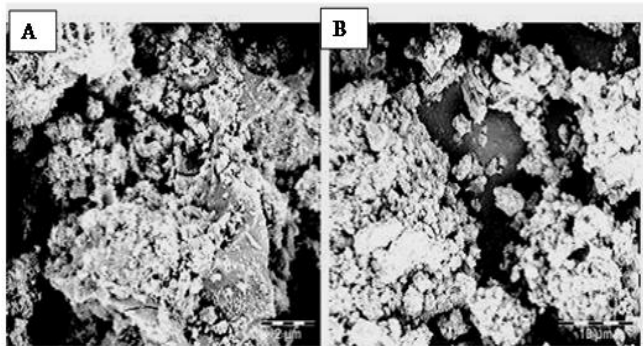


Fig. 9. SEM micrographs of the sludge of the AMD with a combination of clay and  $CaCO_3$  during rapid and slow mixing

The SEM micrograph (Fig. 9) of the sludge of a sample with a combination of bentonite clay and  $MgCO_3$  rapid during mixing (Fig. 9A) and slow mixing (Fig. 9B), where the former shows the agglomeration of moderate dense structures with some small structures scattered around on their surface. On the other hand, the micrograph (Fig. 9B) shows clusters of agglomerates separated by the voids. The structural morphology of the micrograph (Fig. 9A) shows that the sample was subjected to shear stress during mechanical agitation whereas the micrograph (Fig. 9B) shows that the agglomerates clustered in fragments. A common denominator between the two micrographs is their sponge-cake like dense non-spherical structures, which depicts optimal adsorption potential due to their crystal configuration. The dense structures also show some form enlargement which is indicative of adsorption of the turbid materials.

The weight % mineral content of the bentonite clay is shown in Table 4, where  $CO_2$  and FeO represent siderite ( $FeCO_3$ ) and form a larger wt. % (33.2 and 45.3 wt.%) of the total complex compounds contained in both coal/gold mineral composition, and the rest are trace elemental compounds. The particles size (Table 4) also plays a pivotal role during treatment, as larger particles settle due to settling velocity whereas fine particles removal is through chemical treatment.

Table 4. Weight and atomic % of bentonite clay.

Element	Weight%	Weight%	Atomic%	Compound%	Formula	No. of ions
C K	9.07	0.46	16.55	33.22	$CO_2$	2.15
Mg K	0.91	0.08	0.82	1.50	$MgO$	0.11
Al K	1.56	0.08	1.26	2.94	$Al_2O_3$	0.16
Si K	5.06	0.13	3.95	10.82	$SiO_2$	0.51
S K	1.48	0.10	1.01	3.69	$SO_3$	0.13
Ca K	1.14	0.08	0.62	1.60	$CaO$	0.08
Ti K	0.53	0.09	0.24	0.89	$TiO_2$	0.03
Fe K	35.25	0.49	13.84	45.34	$FeO$	1.79
O	45.02	0.58	61.70			8.00
<b>Totals</b>	<b>100.00</b>					

The Pearson correlation coefficient ( $r$ ) is used to calculate the relation between pH and residual turbidity. A correlation coefficient of 0.70 or higher is considered to be a very strong relationship, 0.40-0.69 a strong relationship, and 0.30-0.39 only a moderate relationship. The results of the experiments are used in the calculations below:

$\Sigma x_{\text{floc-rapid/slow}}$  = sum of pH during rapid/slow mixing,  $\Sigma y_{\text{floc-rapid/slow}}$  = sum of turbidity removal during rapid/slow mixing,  $\Sigma x^2_{\text{floc-rapid/slow}}$  = sum of the square of pH during rapid/slow mixing,  $\Sigma y^2_{\text{floc-rapid/slow}}$  = sum of the square of turbidity during rapid/slow mixing and  $\Sigma xy_{\text{floc-rapid/slow}}$  = sum of pH multiplied by sum of turbidity removal (floc = flocculent).

$\Sigma x_{\text{floc-rapid}} = 36.4$ ,  $\Sigma x^2_{\text{floc-rapid}} = 295.5$ ,  $\Sigma y_{\text{floc-rapid}} = 31.4$ ,  $\Sigma y^2_{\text{floc-rapid}} = 472.5$  and  $\Sigma xy_{\text{floc-rapid}} = 151.4$

$\Sigma x_{\text{floc-slow}} = 35.7$ ,  $\Sigma x^2_{\text{floc-slow}} = 291.2$ ,  $\Sigma y_{\text{floc-slow}} = 56.5$ ,

$\Sigma y^2_{\text{floc-slow}} = 815.5$  and

$\Sigma xy_{\text{floc-slow}} = 362.3$

Using the results obtained for the AMD sample with a combination of bentonite clay and  $MgCO_3$  rapid and slow mixing respectively, yielded  $r$ -values of 0.874 and 0.791 (87.4 and 79.1 %), respectively. The range of the correlation coefficient is from -1 to 1 which calculated for the samples with shaking in the present experiment fall within a range of strong and very strong relationship. This is validated the correlation coefficients,  $R^2$  (Figs. 5 and 6) between the pH and turbidity removal efficiencies of the AMD with a combination of bentonite clay and  $MgCO_3$  during rapid and slow mixing respectively, 0.979 and 0.986 (97.9 and 98.6 %), showing that the predictions obtained for the experimental data is considered to be satisfactory.

#### 4. Conclusion

Inorganic coagulants are the most suitable wastewater treatment reagents due to high valence and electronegativity. When added to a colloidal suspension, they cause destabilization which involves the diffusion of the positively charged ions of a metal salt across the EDL and neutralize the electrostatic repulsive forces. The equilibrium which is attributed to the van der Waals attractive and electrostatic repulsive forces shifts and the concentration of positive ions proliferates, causing attraction between neighboring counterionic charges. The size (radius) of the colloidal particles decreases and agglomeration commences. During the process of destabilization-hydrolysis, the rate of mechanical agitation is insignificant as the reactions are mostly influenced by the Brownian motion of the bulk solution. Settling is also predominant due to velocity gradient and differential velocity within the system.

Another factor which influences the rate of the reactions includes the physico-chemical properties of both the colloidal suspension and the reagents. The properties of the colloidal suspension are identified by the type of the colloid (hydrophilic or hydrophobic) whereas those of the reagents vary in accordance with their acidic, basic, valence, electronegativity, amount of internal energies in a reagent,

hydrolysis potential, among others. Acidic reagents, i.e. Fe or Al salts are common due to their abundance on the earth's crust whereas basic are mostly employed for pH adjustment and to depress solubility of the heavy metals in the solution. On the other hand, bentonite clay has also been employed in AMD treatment but the disadvantage is its plasticity and compressibility which may result in the formation of a hard solid material. Combining it with a basic reagent ( $\text{MgCO}_3$ ) will impair that structural transformation as those properties are impaired. The use of such a mixture is appropriate in AMD as the  $\text{MgCO}_3$  elevates the pH, hydrolysis to form  $\text{Mg}(\text{OH})_2$  precipitates (flocs) and adsorbs turbid materials. On the other hand, bentonite clay is predominantly involved in adsorption. The most advantage with Mg is that it can operate up to higher pH values.

The ionic strength and conductivity of the AMD attributable to the dissolved solids is another factor which ameliorates adsorption capacity of the flocculent. Apart from those properties, electrophoretic mobility (V/E) and the zeta potential are some of the factors which determine the amount of dosage required to achieve the best treatment results. However, the considerations for electrophoretic characteristics of colloids and their stability apply only to hydrophobic colloids, the type of the sample treated in this study. Based on the various factors which determine the quality of the treated wastewater, and the complexity of the AMD sample, a choice of the reagent, dosage, method of chemical dispersion and retention time play a pivotal role in wastewater treatment.

The pH of the AMD sample treated in this study was not adjusted mainly due to the high ionic strength of the AMD and the adsorption capacity of bentonite clay and the  $\text{Mg}(\text{OH})_2$ . Destabilization-hydrolysis is highly plausible due to the valence and electronegativity of the  $\text{Mg}^{2+}$ , including the type of the colloid the AMD sample fall under, i.e. hydrophobic nature. In addition, predominant reactions include physical-chemical phenomenon as there are no biodegradable constituents.

The oxygen content of the DO and ORP is not influenced by the rate of mechanical agitation as it does not show significant variation between the raw and treated AMD. Conductivity of the samples with increasing bentonite clay while keeping  $\text{MgCO}_3$  constant decreases with increasing dosage, which is indicative of adsorption of the ions onto the negative sites of the porous bentonite when ionic strength increases.

Bentonite clay controls equilibrium state of the ionic strength of the system through adsorption of excess ions added to the system. This is observed by decreasing conductivity of the samples with increasing bentonite clay while keeping the  $\text{MgCO}_3$  constant and vice versa. The results obtained between the AMD sample treated with rapid and slow mixing respectively, did not exhibit significant deviation which indicates that velocity gradient induced by mechanical agitation does not have an influence on the turbidity removal from the AMD sample using a flocculent.

## References

- Aboulhassan MA, Souabi S, Yaacoubi A, and Bauda M. 2006. Removal of surfactant from industrial wastewaters by coagulation flocculation process. *Interface Journal of Environmental Science & Technology* 3(4): 327-336. DOI: <https://doi.org/10.1007/BF03325941>
- Akcil A. and Koldas S. 2006. Acid minedrainage: causes, treatment and case studies. *J Clean. Prod.* 14: 1139-1145. DOI: <https://doi.org/10.1016/j.jclepro.2004.09.006>
- Aubé B and Arseneault B. 2003. "In-Pit Mine Drainage Treatment System in a Northern Umate" In Proceedings for Sudbury Mining and Environment Conference" available at <http://www.enviaubi.com/images/raglan.pdf>
- Bratby J. 2006. *Coagulants in Coagulation and Flocculation in Water and Wastewater Treatment*, second (ed), IWA Publishing, London, p. 50-68.
- Dzombak DA and Hudson RJM. 1995. In "Aquatic Chemistry: Interfacial and Interspecies Process" (C.P. Huang, C.R. O'Melia and J.J. Morgan, Eds.), p. 59, Am. Chem. Soc. Washington DC. USA. DOI: <https://doi.org/10.1021/ba-1995-0244.ch003>
- EEB. 2000. The environmental performance of the mining industry and the action necessary to strengthen European legislation in the wake of the Tisza-Danube pollution, European Environmental Bureau, Document No. 2000/016, p. 32.
- Ekosse G-IE, Jumbam ND. 2010. Geophagic clays: their mineralogy, chemistry and possible human health effects. *Afri. J Biotechnol.* 9: 6755-6767.
- Emmanuel IU, Jens CW, Lubahn S and Taubert A. 2013. Hybrid Clay: A New Highly Efficient Adsorbent for Water Treatment, *Chem. Eng.* 1 (8) : 966-973.
- Gitari WM, Kaseke C, and Nkuzani BB. 2011. Passive Remediation of Acid Mine Drainage using Bentonite Clay: A Laboratory Batch Experimental Study. *Int. Mine Wat. Asso.* 325-330.
- Kurniawan TA, Chan WS, Lo WH, and Babel S. 2006. Physico-chemical treatment techniques for wastewater laden with heavy metals. *J. Chem. Eng.* 118: 83-87. DOI: <https://doi.org/10.1016/j.cej.2006.01.015>
- Mail & Guardian. 2005. A rising acid tide by Mellisa Fourie, 12 April 2005.
- Pulles W, Banister S, and van Biljon M. 2005. The development of appropriate procedures towards and after closure of underground gold mines from a water management perspective, Report No. 1215/1/05, Wat. Res. Com. Pretoria, South Africa.
- Mansri A, Bendraoua A, Benmoussa A, and Benhabib K. 2015. New Polyacrylamide [PAM] Material Formulations for the Coagulation/Flocculation/Decantation Process, *J. Polymer and Environ.* 23 (4): 580-587. DOI: <https://doi.org/10.1007/s10924-015-0734-7>
- Maree JP. 2004. Treatment of industrial effluent for neutralization and sulphate removal; A thesis submitted for PhD at the North West University, RSA.
- Nagajyoti PC, Lee KD, and Sreekanth TVM. 2010. Heavy metals, occurrence and toxicity for plants: a review. *Environ. Chem.* 8: 199-216. DOI: <https://doi.org/10.1007/s10311-010-0297-8>
- Nel M, Waander FB, and Fosso-Kankeu E. 2014. Adsorption potential of bentonite and attapulgite clays applied for the desalination of sea water. Conference Report. Cape Town: 6th International Conference on Green Technology,

- Renewable Energy & Environmental Engineering North-West University.
- Ntwampe IO, Jewell LL, and Glasser D. 2013. The effect of mixing on the treatment of paint wastewater with  $\text{Fe}^{3+}$  and  $\text{Al}^{3+}$  salts. *J. of Environ. Chem. and Ecotoxicol.* 5(1): 7-16.
- Ntwampe IO, Waanders FB, Fosso-Kankeu E, and Bunt JR. 2015a. Turbidity removal efficiencies of clay and af-PFCl polymer of magnesium hydroxide in AMD treatment, *Int. J Sci. Res.* 4: 38-55.
- Ntwampe IO, Waanders FB, and Bunt JR. 2015b. Optimization of a polymeric reagent of clay and varying concentrations of  $\text{FeCl}_3$  with dolomite dosage in AMD treatment, submitted to *J. Mine Wat. and Environ.* [Unpublished].
- Ntwampe IO, Waanders FB, and Bunt JR. 2016. Destabilization dynamics of clay and acid-free polymers of ferric and magnesium salts in AMD without pH adjustment, *Wat. Sci. & Technol.* 74, 4: 861-875. DOI: <https://doi.org/10.2166/wst.2016.259>
- Ouazene N. 2010. Equilibrium and kinetic modeling of astrazonyellow adsorption by sawdust: effect of important parameters. *Int J Chem React Eng.* DOI: <https://doi.org/10.2202/1542-6580.2413>
- Oladipo A A, Gazi M. 2014. 'Enhanced removal of CV by low cost alginate/acid activated bentonite composite beads; Optimization and modeling using non-linear regression technique', *J. of Wat. Proc. Eng.* 2: 43-52. DOI: <https://doi.org/10.1016/j.jwpe.2014.04.007>
- Otto CC and Haydel SE. 2013. Microbial clays: composition, activity, mechanisms of action and therapeutic applications, A. Méndez-Vilas, ed. In: *Microbial pathogens and strategies for combating them: science, technology and education.* Badajoz, Spain: Formatex Research Center. 2: 1169-1180.
- Sincero AP and Sincero GA. 2003. *Physical-chemical treatment of water and wastewater*, IWA Publishing, Londaio, USA.
- Syafalni, Abdullah R, Abustan I, Ibrahim ANM. 2013. 'Waste water treatment using bentonite, the combination of bentonite-zeolite, bentonite-alum, and bentonite-limestone as adsorbent and coagulant. *Int. J Environ. Sci.* 4 (3): 2013.
- Swartz CD and Ralo T. 2004. Guidelines for planning and design of small water treatment plants for rural communities with specific emphasis on sustainability and community involvement and participation, Silowa Printers, SA.
- Tahir SS and Naseem R. 2007. Removal of  $\text{Cr}^3$  from tannery waste water by adsorption onto bentonite clay. *Sep. and Purific. Technol.* 53: 312-321
- Waanders FB and Brink MC. 2010. The Rehabilitation of Acid Mine Effluents and Toxic Heavy Metal Pollution, emanating from gold mines in South Africa, Proceedings XXV International Minerals processing Conference, IMPC-2010, Brisbane, Australia, 4117-4126.

*Conflict of interest: Non declare*